American Mineralogist, Volume 81, pages 696–705, 1996

Modification of garnet by fluid infiltration during regional metamorphism in garnet through sillimanite-zone rocks, Dutchess County, New York

DONNA L. WHITNEY,[1] TRUDY A. MECHUM,[1,*] YILDIRIM DILEK,[2] AND SCOTT M. KUEHNER[3]

[1]Department of Geology, University of North Carolina, Chapel Hill, North Carolina 27599, U.S.A.
[2]Department of Geology and Geography, Vassar College, Poughkeepsie, New York 12601, U.S.A.
[3]Department of Geological Sciences, University of Washington, Seattle, Washington 98195, U.S.A.

ABSTRACT

Metapelitic rocks from a progressive metamorphic sequence in Dutchess County, New York, record evidence for reaction between garnet and fluids associated with quartz (±plagioclase) veins and for net transfer among garnet interiors, mineral inclusions, and fluid. Garnet-fluid reaction resulted in modification of preexisting garnet textures, compositions, and growth-zoning patterns.

The textural and compositional record of garnet-fluid interaction varies with grade and with proximity of garnet to quartz veins. Garnet-zone rocks do not contain evidence for extensive reaction with vein-forming fluids. In upper staurolite- and kyanite-zone rocks, garnet that is crosscut by quartz veins contains a fluid-inclusion–filled region near the garnet-vein interface. This region truncates growth-zoning patterns and quartz inclusions. Fluid inclusions in garnet decrease in abundance away from quartz veins. In some rocks lacking quartz veins, fluid inclusions are concentrated in garnet interiors, and in particular near fractures, and are notably lacking around mineral inclusions in garnet.

Inferences from textural and compositional features combined with thermobarometric results indicate that preexisting garnet grains were modified at $T \approx 525$–550 °C and >4 kbar by one or more reactions involving fluids. The fluid pathways included foliation-parallel channels in the rock as well as microcracks in mineral grains.

INTRODUCTION

Fluids drive mineral reactions, transport heat and solutes, and affect deformational mechanisms during metamorphism. Numerous investigations have used mineralogic, stable isotopic, or other chemical indicators to document the extent and effects of fluid infiltration during regional metamorphism (e.g., Rumble 1989; Ferry and Dipple 1991). Textural evidence for passage of fluid through the crust during regional metamorphism includes metasomatic reaction zones and veins (commonly quartz rich). Numerous studies have documented chemical and isotopic alteration of metacarbonates associated with vein-forming fluids (e.g., Tracy et al. 1983). Quartz veins in metapelitic rocks, however, are not commonly reported to show evidence for reaction with phases in the host rock (Yardley and Bottrell 1992).

Garnet typically records compositional and, in some cases, textural evidence for changing *PTX* conditions during metamorphism. There is abundant evidence that prograde garnet compositions and zoning patterns may be modified by a variety of processes. Volume diffusion and the subsequent homogenization of growth zoning are the expected effects of metamorphism at high temperatures (>600 °C; e.g., Loomis et al. 1985). In addition, growth zoning may be perturbed by exchange reactions between garnet and Fe-Mn-Mg–rich matrix phases and mineral inclusions (biotite, ilmenite, chloritoid) during prograde (Whitney and Ghent 1993) or retrograde (Tracy 1982) reaction.

Prograde garnet compositions may also be modified by reactions involving phases external to the garnet. Whitney (1991) demonstrated that plagioclase inclusions in garnet from a sillimanite gneiss had participated in high-temperature retrograde net-transfer reactions involving the inclusions, host garnet, and phases in the groundmass of the rock (±fluid). Hames and Menard (1993) described metasomatic modification of garnet at the rim, along cracks, and at mineral-inclusion boundaries and presented textural evidence for involvement of a fluid. Erambert and Austrheim (1993) and Ague (1995) presented evidence for modification of garnet composition along fractures, and proposed that perturbation of preexisting garnet composition occurred in response to fluid infiltration. The Barrovian sequence that is the focus of the present

* Present address: Department of Geological Sciences, University of Texas, Austin, Texas 78712, U.S.A.

0003-004X/96/0506-0696$05.00

study provides new information about the postcrystallization modification of garnet because evidence for the paleo-fluid pathways is preserved in textural and compositional features in garnet.

Geological background

The samples described in this paper are from a progressive metamorphic sequence in Dutchess County, southeastern New York. This sequence consists of unmetamorphosed through sillimanite–potassium feldspar-zone metasedimentary rocks extending ~30 km from the easternmost unmetamorphosed locality near the Hudson River to the second sillimanite isograd near the New York–Connecticut border (Fig. 1a). The protoliths are Cambrian and Ordovician sandstone, shale, and carbonates.

The petrology and structural geology of the area were described in detail by Barth (1936) and Balk (1936). Garlick and Epstein (1967) obtained O isotope data for rocks from the garnet through sillimanite zones and calculated a temperature range of 480–625 °C using their isotopic data. Vidale (1974) remapped isograds proposed by Barth (1936) using petrographic rather than field observations of the first appearance of index minerals and described changes in vein mineralogy with increasing metamorphic grade (see also Vidale 1973). The most recently published studies of the geology of Dutchess County are field guides by Bence and McLelland (1976), McLelland and Fisher (1976), and Fisher and Warthin (1976), a map and accompanying text by Ratcliffe and Burton (1990), and a thermobarometric study (Whitney et al. 1996).

Hames et al. (1991), in the most recent geochronologic study of the area, used $^{40}Ar/^{39}Ar$ dating of micas to determine an age of ~445 Ma for the Taconic staurolite zone and delineated an area in which Acadian metamorphism at 390–400 Ma partially overprinted some Taconic textures and mineral-rim compositions (Fig. 1a). According to Hames et al. (1991), the easternmost part of the Dutchess County sequence may have been affected by Acadian thermal events; localized regions of Acadian deformation may occur as far west as the Hudson River.

Petrography and mineral compositions

Mineral analyses were obtained using a Cameca Camebax electron microprobe at Duke University. X-ray maps of garnet were generated with a JEOL 733 electron microprobe at the University of Washington. X-ray intensities were digitized using the GATAN Digital-Micrograph system.

Garnet zone

Garnet-zone rocks contain garnet + biotite + quartz + plagioclase + muscovite ± chlorite ± chloritoid + ilmenite + graphite + tourmaline. Quartz veins are abundant. Many parallel foliation but some cut across and locally truncate foliation. Veins range in thickness from <1 mm to 4–5 cm and commonly show pinch and swell structures along strike. Some veins are ptygmatically folded. Inclusions of wall-rock minerals (biotite, chlorite, garnet) occur within veins. Quartz occurs as polygonal aggregates; most grains are large, strain-free crystals with dihedral angles, but some anhedral grains are present and exhibit undulatory extinction. Locally, radial chlorite fibers have overgrown large quartz grains.

Garnets in pelitic samples are idiomorphic, ~1 mm in diameter, contain geometric arrays of fine-grained mineral inclusions (mostly graphite), and exhibit concentric growth-zoning patterns (Fig. 2a). Garnet cut by veins displays truncated but otherwise normal growth zoning (Fig. 2b). Zoning profiles in both intact (Fig. 2c) and truncated (Fig. 2d) garnet show a slight discontinuity in zoning within 100–250 μm of the vein. Biotite also appears to be truncated by quartz veins, but no compositional trends in relation to vein proximity are apparent.

Staurolite zone

Most staurolite-zone rocks contain the assemblage garnet + biotite + muscovite + staurolite + quartz + plagioclase ± chloritoid + ilmenite + graphite + tourmaline. Chloritoid is present in lower staurolite zone rocks with Al- and Fe-rich bulk composition in the western part of the staurolite zone but shows textural evidence for replacement by staurolite. In some samples from the eastern part of the zone, large staurolite poikiloblasts (up to 1 cm long) contain idiomorphic inclusions of garnet (~1 mm in diameter), and garnet contains inclusions of staurolite.

The sample shown in the photomicrographs (Fig. 3) is from the upper (eastern) staurolite zone and consists primarily of large (1–1.6 mm), rounded to subidiomorphic garnet grains in a matrix dominated by muscovite (X_{Na} = 0.14–0.19) that defines a well-developed crenulated foliation. Staurolite (up to 5 mm), biotite, quartz, plagioclase, ilmenite, and zoned idiomorphic tourmaline are also present. Garnet contains inclusions of quartz, plagioclase, ilmenite, apatite, and tourmaline in core regions but has rims free of mineral inclusions (Fig. 3). Plagioclase inclusions, some of which are faceted (negative crystals), are zoned, with anorthite content increasing from core to rim. Typical values for apparent core-to-rim variation are $\Delta X_{An} \approx 5$–10 mol%, although inclusions with core-to-rim variation of up to 35 mol% anorthite are present. Garnet composition decreases in Ca and Mn and increases in Fe and Mg in the vicinity of reverse-zoned plagioclase inclusions (cf. Whitney 1991).

Some samples are cut by a series of ~1 mm wide stretched and ptygmatically-folded veins consisting primarily of quartz, with lesser amounts of plagioclase, muscovite, and apatite. Vein plagioclase exhibits strong normal zoning ($X_{An,core}$ = 0.26, $X_{An,rim}$ = 0.14). In contrast, matrix plagioclase grains are homogeneous or have slightly normal zoning ($X_{An} \approx 0.18$). Fluid-inclusion trails in vein quartz are oriented perpendicular to the trend of the vein.

Veins are parallel to one direction of muscovite growth in the matrix but at an ~20° angle to a second direction. The two directions of mica growth form the crenulation fabric. Vein growth is typically parallel to compositional banding in the rock; the banding is defined by alternating mica-rich and staurolite-rich layers. Quartz veins are most abundant in the former.

Some veins include slivers of wall rock oriented parallel to the vein walls. Quartz is generally strain free and has dihedral angles, although the degree of recrystallization is not as high as in veins in garnet-zone rocks. Veins crosscut and truncate garnet, chloritoid, staurolite, and biotite. Where the veins crosscut garnet, a texturally distinct garnet zone (~75–300 μm wide) is present along the garnet-vein contact (Figs. 3a–c). These zones truncate quartz (but not ilmenite) inclusions in garnet and contain abundant fluid inclusions. Some fluid inclusions are preserved in linear zones oriented perpendicular to the trend of the adjacent quartz vein (Figs. 3a and 3b). Fluid inclusions are also present in the core of the garnet but decrease in abundance with increasing distance from the vein.

Garnet that is not crosscut by veins (e.g., Figs. 3d and 4a) displays normal growth zoning, with Fe increasing from core to rim (X_{Alm} = 0.53–0.80), Ca and Mn decreasing from core to rim (X_{Grs} = 0.17–0.03, X_{Sps} = 0.28–0.07), and Mg constant throughout most of the core region (X_{Prp} = 0.03) but increasing near the rim (X_{Prp} = 0.11). Garnet cores are spessartine rich, with $X_{Alm} > X_{Sps} > X_{Grs} > X_{Prp}$, except in near-rim regions where pyrope exceeds the spessartine and grossular components.

Garnet crosscut by veins also shows normal growth zoning in the interior region, but this zoning is truncated near the vein. Over a distance of ~75–300 μm in the texturally modified zone, Fe and Mg decrease away from the rim (up to 0.13 ΔX_{Alm}) and Mn and Ca increase (Figs. 3e and 3f). It is remarkable that some texturally modified zones adjacent to quartz veins have sharp, straight boundaries within garnet (Figs. 3a and 3b). X-ray maps of garnet, however, illustrate that the textural boundary does not everywhere coincide with a compositional boundary and that elemental distributions in the modified zone follow the irregular shape of the garnet margin in contact with the quartz vein (Fig. 4b).

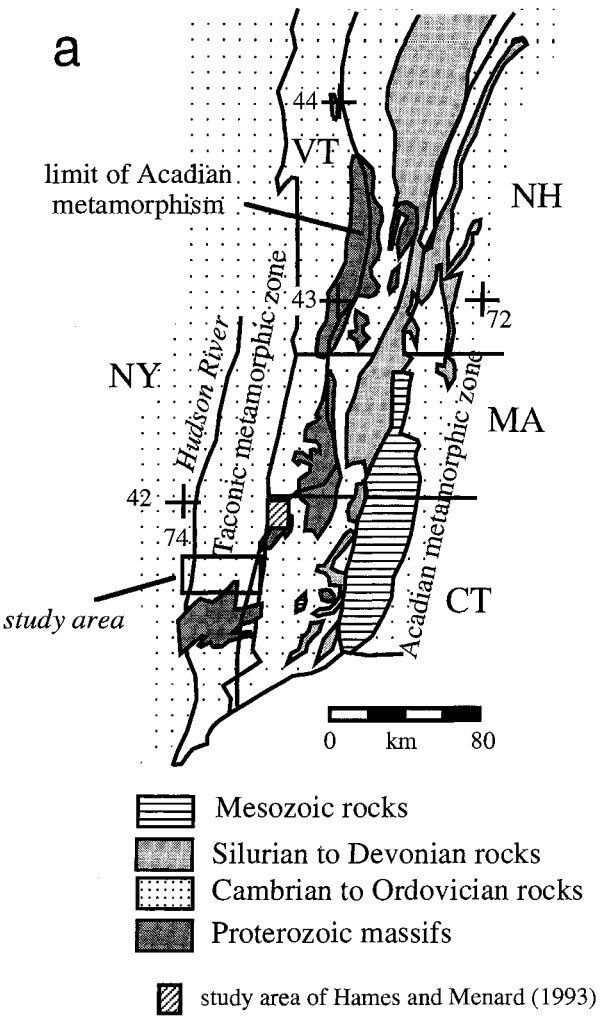

FIGURE 1. (a) Regional map showing the location of the study area. The limit of Acadian metamorphism is from Hames et al. (1991). (b) Map of Dutchess County with isograds and sample localities (geology modified from Fisher et al. 1970).

Kyanite zone

Most kyanite-bearing metapelitic rocks contain the assemblage garnet + biotite + muscovite + quartz + plagioclase + kyanite ± staurolite + ilmenite ± rutile ± tourmaline. Some kyanite-bearing samples collected for this study contain trace amounts of fibrolite along kyanite rims and associated with biotite. The first appearance of kyanite in the sequence coincides with the first appearance of fibrolite [cf. isograd maps of Barth (1936) and Vidale (1974)] (Fig. 1b).

In kyanite-bearing samples, garnet is typically idioblastic to subidioblastic with small embayments occupied by quartz or plagioclase ± fibrolite. Whitney et al. (1996) proposed that the presence of clusters of fibrolite along garnet margins where the rim has been embayed by plagioclase suggests that the fibrolite was produced by a garnet resorption reaction rather than being a reactant. Matrix plagioclase grains and plagioclase adjacent to garnet are essentially homogeneous (An_{23-25}). Where garnet rims are not embayed, biotite is typically adjacent to the garnet rim.

Some matrix garnets contain a nearly homogeneous core (~500–600 μm in diameter) but display normal growth zoning from the outer core to the rim; $X_{Alm} \geq X_{Sps} > X_{Grs} \geq X_{Prp}$ in garnet core regions, and $X_{Alm} \gg X_{Sps} > X_{Prp} > X_{Grs}$ in near-rim regions (Fig. 5a). The boundary between the inclusion-filled core and inclusion-free rim regions corresponds to a discontinuity in zoning: X_{Alm} continues to increase, but the concentration profiles steepen toward

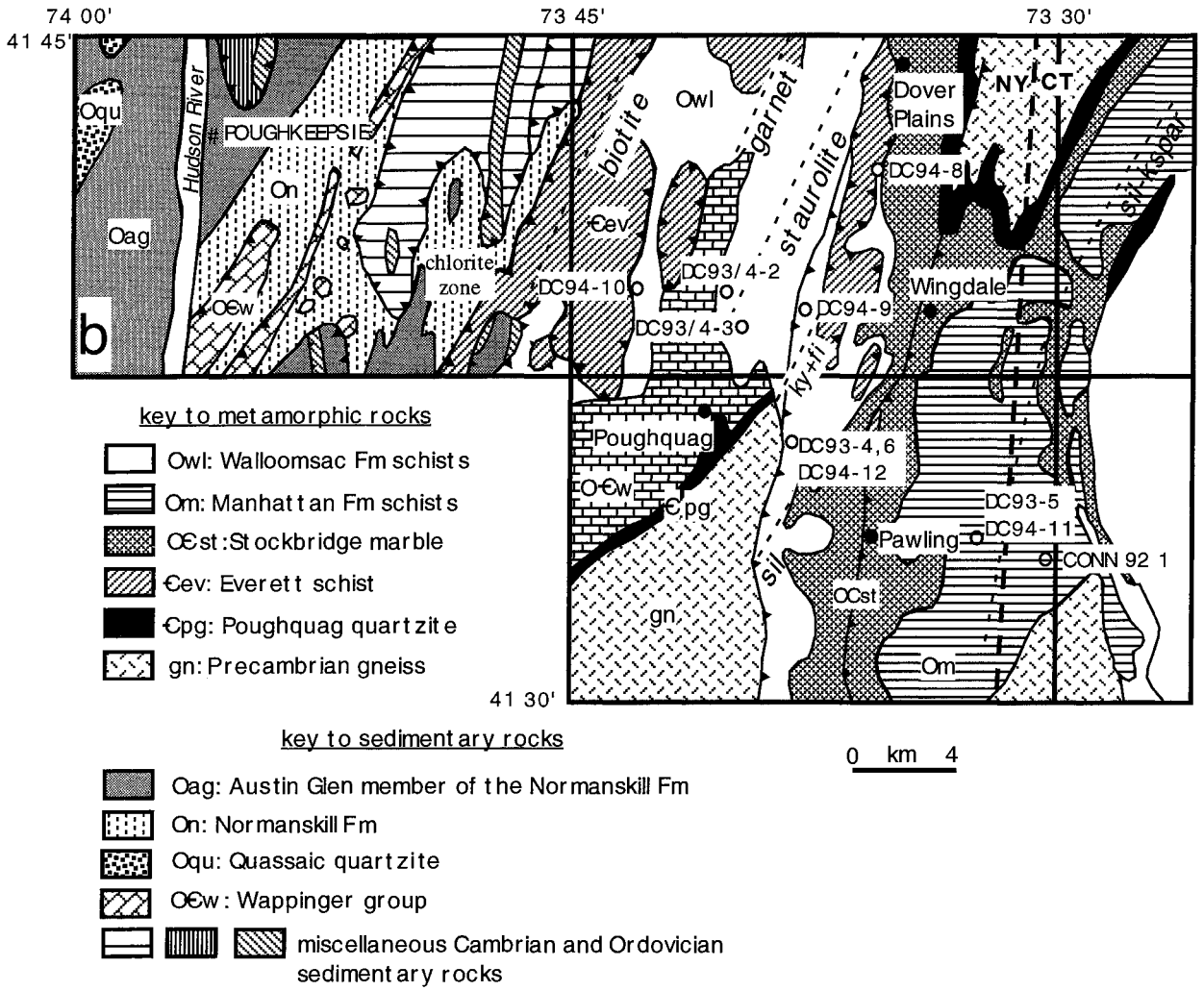

FIGURE 1.—*Continued*

the rim; X_{Sps} is essentially homogeneous; X_{Grs} decreases; and X_{Prp} is homogeneous in a vein, it is disaggregated and clouded by abundant fluid inclusions, and the rim is highly embayed and locally altered to biotite.

Mineral inclusions in garnet are quartz, biotite, plagioclase, tourmaline, rutile, Mn-rich ilmenite, muscovite, and zircon. In some samples, garnet cores are entirely replaced by biotite and quartz. Intact garnet cores contain a high concentration of very fine-grained inclusions, which appear to be fluid inclusions, graphite, quartz, apatite (?), and rutile (?).

The distribution of fluid inclusions in garnet varies from sample to sample. In some samples, fluid inclusions are distributed throughout the core region. In others, fluid inclusions are arranged in arrays that resemble healed fluid-inclusion–bearing microcracks. Some arrays are parallel to each other. These parallel linear features may represent slices through fluid-inclusion–rich internal schistosity surfaces overgrown by garnet (R. Tracy 1995, personal communication). Regardless of fluid-inclusion distribution, all garnets contain an inclusion-free rim.

In some samples, garnet contains inclusion-free zones around mineral inclusions (e.g., biotite, quartz; Figs. 5c and 6), and the inclusion-free zone is surrounded by a greater concentration of fine-grained inclusions (primarily fluid inclusions) than is present in the rest of the host garnet (Fig. 5c). Visible cracks in garnet are also surrounded by zones of high concentration of fluid inclusions. Garnets adjacent to centimeter-scale quartz veins contain linear zones of fluid inclusions that are oriented perpendicular to the garnet-vein interface (Fig. 5d).

Sillimanite (fibrolite) zone

The distinction between the kyanite and sillimanite (fibrolite) zones is not well defined because fibrous sillimanite (fibrolite) is present in trace amounts in most kyanite-bearing samples. Samples designated as sillimanite zone contain abundant fibrolite as well as trace amounts

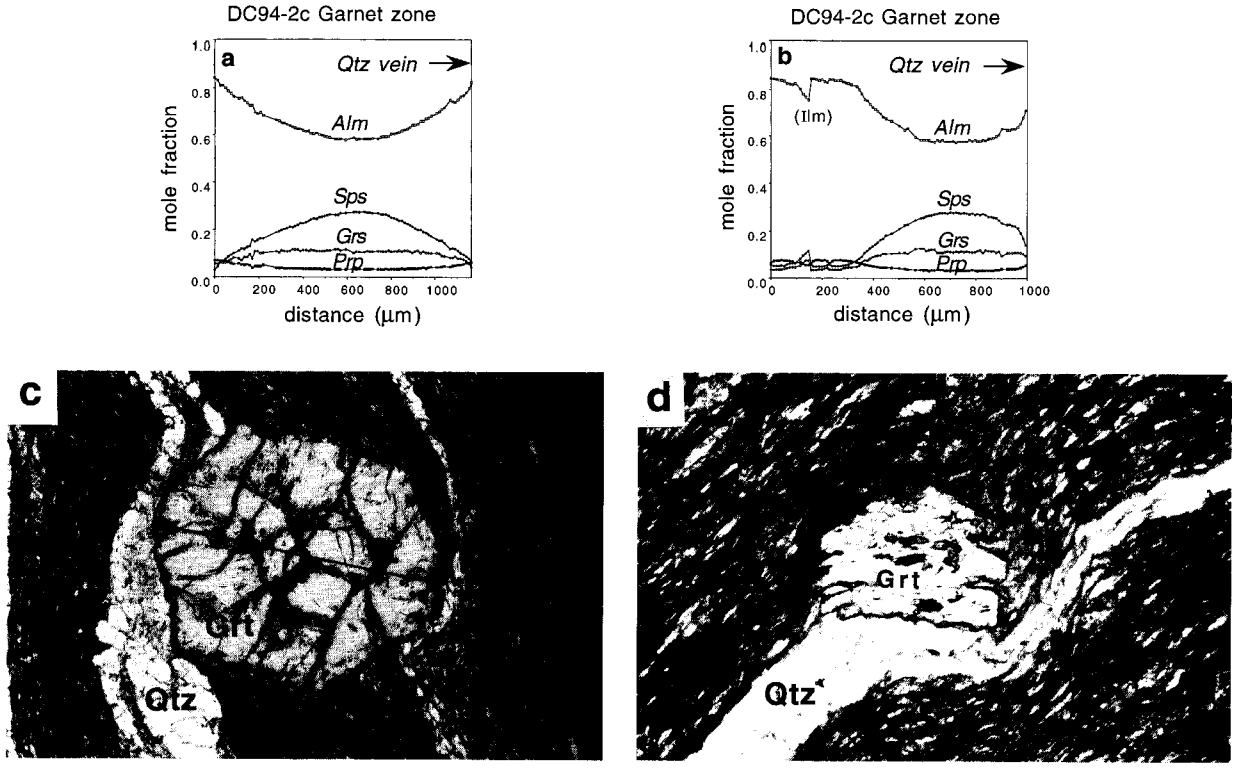

FIGURE 2. Garnet zoning (**a** and **b**) and photomicrographs from garnet-zone sample DC94-2c. (**c**) Garnet + quartz vein. The arrow indicates the path of the microprobe traverse shown in **a**. Field of view = 2 mm. (**d**) Truncated garnet from the same thin section. Beyond the field of view, the quartz vein is ptygmatically folded. Field of view = 0.75 mm. Mineral abbreviations after Kretz (1983).

of coarse, prismatic sillimanite. Sillimanite zone rocks typically contain the assemblage garnet + biotite + muscovite + quartz + plagioclase + sillimanite or fibrolite + ilmenite ± staurolite ± kyanite + tourmaline.

Some samples contain 10–15 vol% fibrolite in large mats and in sprays within matrix plagioclase, quartz, and muscovite, and within quartz inclusions in garnet. Staurolite is present as inclusions in garnet near-rim regions and persists as a matrix phase. Some garnet grains in this sample lack the fine-grained mineral and fluid inclusions present in most other sillimanite-zone samples; other garnet grains in the same thin section contain 100–300 μm wide bands of negative crystal microinclusions. Garnet cores are essentially unzoned (Fig. 7).

PRESSURE-TEMPERATURE CONDITIONS

Metamorphic pressure-temperature conditions range across the sequence from ~475 °C and 3–4 kbar in the garnet zone to >720 °C and ~5–6 kbar in the sillimanite–potassium feldspar zone (Whitney et al. 1996). These values were determined using the garnet-biotite geothermometer [Ferry and Spear (1978); Hodges and Spear (1982) and Berman (1990) garnet model] and garnet-plagioclase-Al_2SiO_5-quartz (GPAQ: Koziol and Newton 1988; Hodges and Crowley 1985) and other geobarometers. Pressures and temperatures determined from garnet outer core, matrix biotite, and plagioclase core compositions (or unzoned plagioclase inclusions in garnet) are typically 1 kbar and ~50 °C higher than those determined from garnet rim, neighboring biotite, and plagioclase rim compositions. Details of the thermobarometric study are in Whitney et al. (1996).

FLUID INCLUSIONS

Fluid inclusions are present in vein quartz and in garnet in upper staurolite- through sillimanite-zone rocks. No fluid inclusions were observed in equant, recrystallized quartz in veins in garnet-zone rocks or in deformed quartz veins in higher-zone rocks. Less-deformed veins in staurolite-zone rocks contain pseudosecondary trails of aqueous and H_2O-CO_2 inclusions in quartz.

Most fluid inclusions observed, both in veins and in garnet, are extremely small (<2 μm). Microthermometric analysis of a limited number of relatively large aqueous inclusions (3–6 μm) in vein quartz determined salinities of ~5.5 wt% NaCl and homogenization temperatures ranging from 150 to 215 °C for inclusions in the same vein.

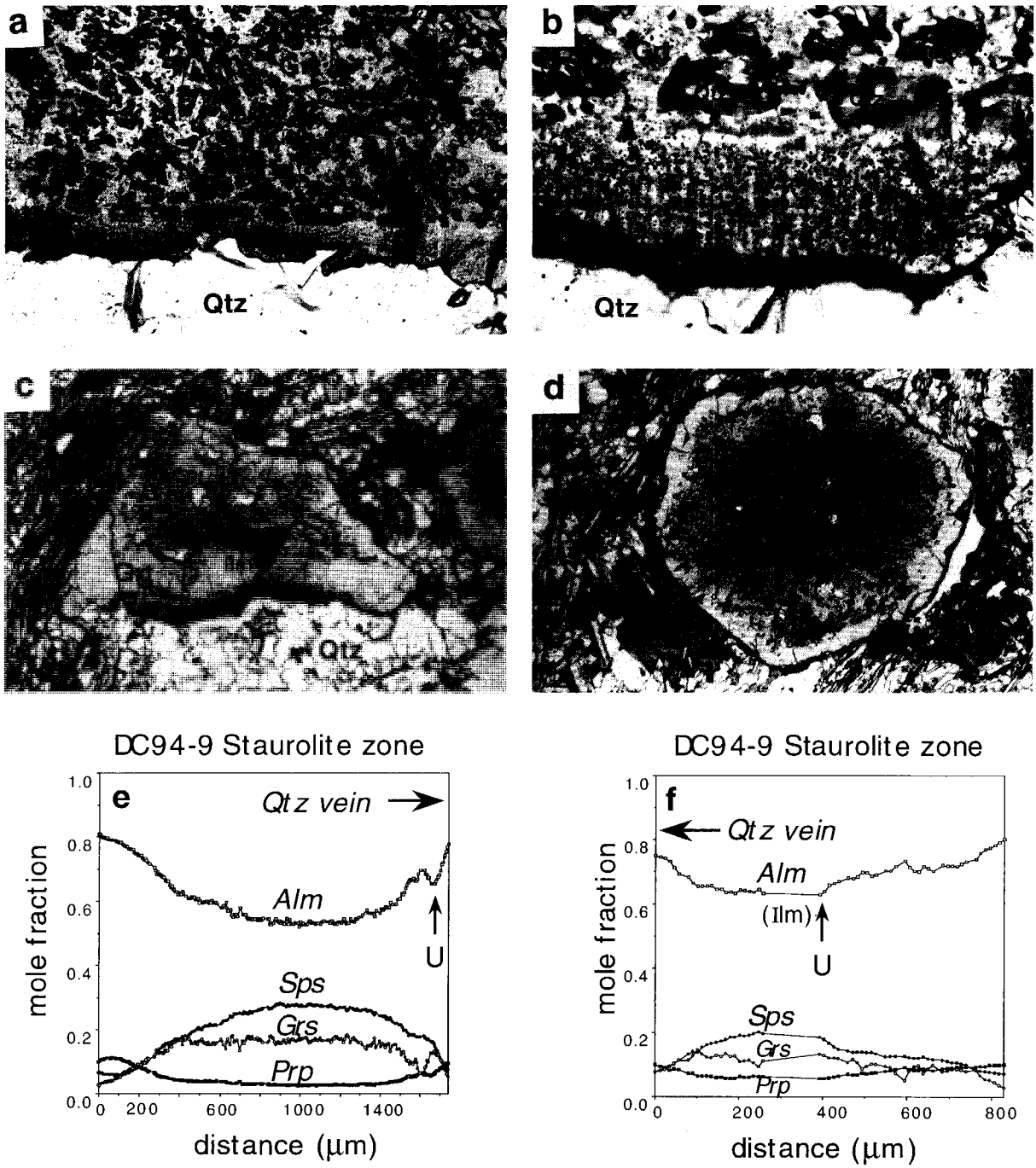

FIGURE 3. Staurolite-zone sample DC94-9. (**a**) Reaction texture between garnet and quartz vein. A fluid-inclusion–filled zone occurs at the contact between garnet and vein, an area free of quartz inclusions. Zoning profile given in **e**. Field of view = 2 mm. (**b**) View of inclusion-rich zone at higher magnification. Note the distribution of fluid inclusions in numerous linear zones perpendicular to the garnet-vein contact. Field of view = 0.75 mm. (**c**) Garnet-vein reaction texture. The cloudy area in garnet near the quartz vein contains abundant fluid inclusions. Field of view = 2 mm. Zoning profile given in **f**. (**d**) Matrix garnet from the same thin section as **a**–**c**. Field of view = 2 mm. (**e** and **f**) Zoning in upper staurolite-zone garnet. Arrows and the symbol U (=unconformity) designate locations of textural boundaries as shown in **a**–**c**.

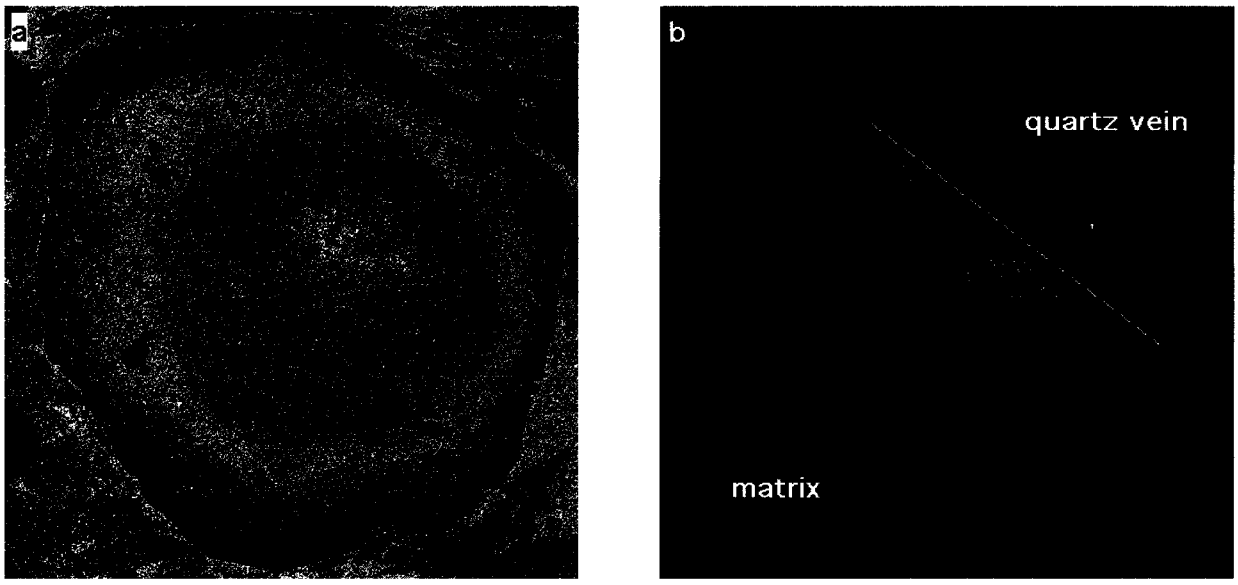

FIGURE 4. X-ray maps of Mn concentration in garnet from upper staurolite-zone sample DC94-9. (a) Matrix garnet. Garnet diameter is ~1.5 mm. (b) Garnet intersected by quartz vein. The dashed white line indicates the textural unconformity defined by truncated quartz inclusions (see Figs. 3a, 3b, and 3e). Field of view = ~2 mm.

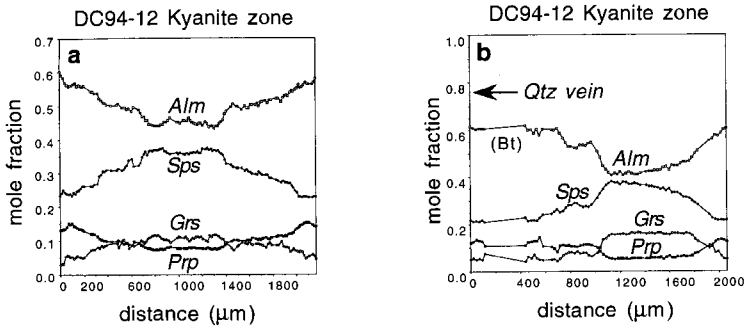

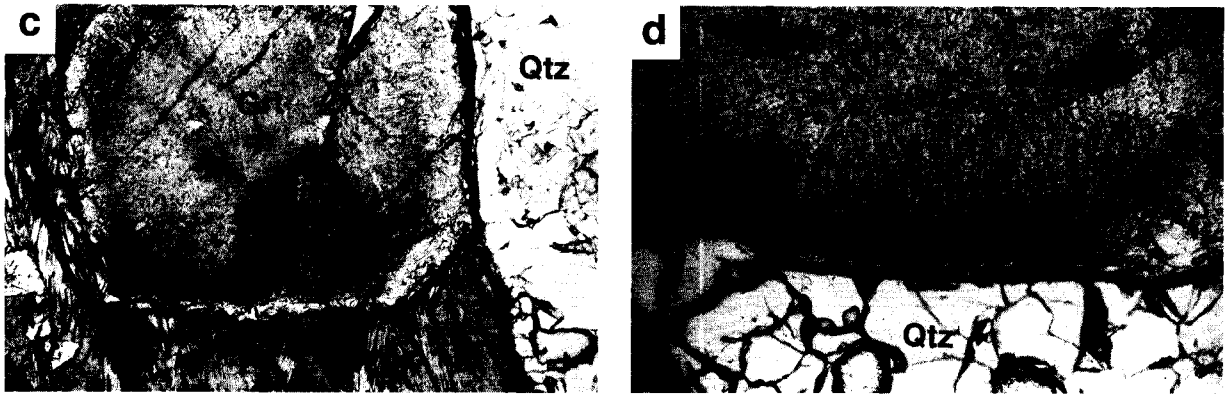

FIGURE 5. Kyanite-zone sample DC94-12. This thin section contains abundant kyanite and minor fibrolite along kyanite rims. (a and b) Garnet zoning. (c) Garnet adjacent to a quartz vein. The biotite inclusion is surrounded by a thin clear (inclusion-free) zone, which is itself surrounded by a zone of greater concentration of graphite and fluid inclusions relative to the rest of the garnet. The near-rim region of the garnet is largely inclusion free but is surrounded by a zone containing a high concentration of fluid inclusions. Field of view = 2 mm. (d) Garnet from the same thin section as a adjacent to a quartz vein. The linear features approximately perpendicular to the quartz vein are arrays of fluid inclusions. Field of view = 0.75 mm.

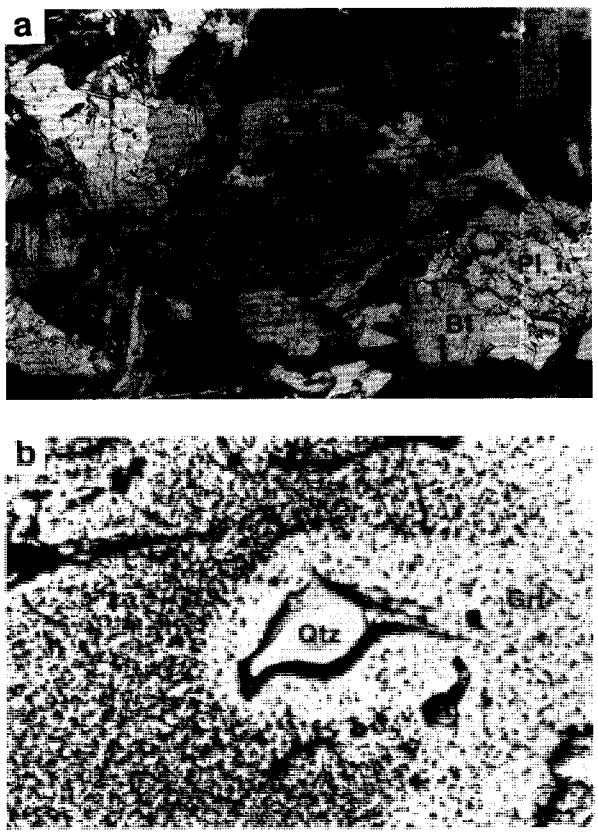

FIGURE 6. Kyanite-zone sample DC93-6. Fluid inclusions are not confined to trails, and garnet is not located near veins. (a) Garnet with inclusion-filled core and inclusion-free rim region. Note the clear zones around mineral inclusions. Field of view = 2 mm. (b) Clear zone around quartz inclusion from another garnet in the same thin section. Field of view = 0.25 mm.

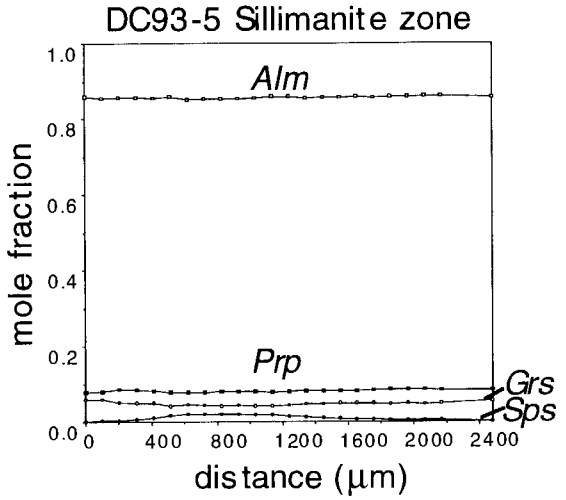

FIGURE 7. Microprobe traverse of a sillimanite-zone garnet.

Fluid inclusions in trails in garnet near the garnet-vein contact are too small (≤ 1 μm) for microthermometric analysis. A few larger (3–9 μm), isolated inclusions near garnet rims in staurolite- and kyanite-zone rocks contain high-density ($T_h = -39$ °C), CO_2-rich inclusions. The origin of these inclusions in relation to garnet growth and modification is not known. If these inclusions were trapped at the same time that the garnet rim formed or equilibrated with adjacent phases, the high density of the inclusions implies trapping at 5–6 kbar.

DISCUSSION

Quartz veins in garnet-zone rocks truncate garnet, but there are no apparent reaction textures or fluid inclusions in these garnets. There appears to have been a slight compositional modification of garnet as evidenced by a break in slope in the zoning profiles adjacent to quartz veins (Figs. 2a and 2b). These observations suggest that the primary effect of veining was the physical disaggregation of garnet. Any chemical reaction that occurred only affected the outer ~100–250 μm of the garnet.

Staurolite- and higher-zone rocks record more dramatic evidence for reaction involving garnet, fluid, and mineral inclusions in garnet. Textural and chemical modification indicating extensive interaction between garnet and fluid increases with proximity of a garnet grain to a quartz vein. Where garnet is completely surrounded by a vein, it is highly embayed and clouded by fluid inclusions. Garnet adjacent to a vein contains fluid inclusions concentrated in the part of the garnet closest to the vein. In most (but not all) rocks examined, garnet grains not touching veins either lack fluid inclusions or do not contain as many fluid inclusions as those in contact with a vein.

Some matrix garnet that lacks fluid inclusions contains reverse-zoned plagioclase inclusions surrounded by zoning halos. The presence of these features indicates net-transfer reaction occurred within garnet after entrapment of plagioclase as an inclusion. Although not required, intergranular fluid probably assisted with local modification of garnet composition around inclusions (Whitney 1991).

Garnet truncation at vein margins indicates that 30–60% of the volume of some garnet grains has been removed by chemical processes, mechanical processes, or both. Garnet-fluid interaction may have involved local dissolution of garnet, but it is likely that mechanical processes were responsible for much of the removal. Evidence for mechanical incorporation of wall rock is found at all grades, and veins in kyanite-zone rocks contain fragments of garnet and kyanite. The fluid-inclusion–filled zones in garnet next to quartz veins may have formed as overgrowths on truncated garnet, or they may represent preexisting garnet in which reaction proceeded inward from the garnet-vein contact.

If large-scale dissolution occurred along vein margins, it is likely that relatively insoluble minerals would be concentrated there. Point counting of upper staurolite-zone thin sections, however, does not indicate any significant change in the mode of the host rock in the vicin-

ity of the veins. Figure 3c illustrates that ilmenite inclusions in garnet were not texturally affected by modification of the near-vein region of the garnet, although quartz inclusions have disappeared from this zone. If this same process were operating in the matrix, ilmenite would probably be concentrated near veins. Furthermore, there does not seem to be evidence for hydration (e.g., of plagioclase) having occurred in the vicinity of veins because the modal percentage of muscovite and biotite is the same near veins and at a distance from veins. However, given the abundance of small-scale veins in most outcrops, it is possible that chemical changes were pervasive and the mode would not be expected to change with proximity to individual veins.

Some sillimanite-zone samples show evidence for metasomatic alteration. These contain 10–15 vol% fibrolite in the matrix and lower modal amounts of micas than other sillimanite-zone metapelitic rocks. The extremely high abundance of fibrolite may indicate that this rock has been enriched in Al and depleted in alkalis (cf. Ague 1994a, 1994b).

The observation that fluid inclusions in garnet adjacent to veins are confined to linear zones (possibly healed cracks or dislocations) and are also spatially associated with visible cracks in garnet suggests that the fluid inclusions are secondary rather than primary. In addition, although the fluid may have been largely channelized along fractures or shear zones in the rock (now represented by veins), fluid infiltration beyond the veins extended into the interior of garnets over distances of at least 1 cm from veins. The presence of fluid inclusions in apparent healed microcracks in garnet in unveined rocks suggests that some (early?) pathways of fluid flow were not associated with precipitation of quartz in veins.

The source of the fluid may have been external or internal to the metapelitic rocks. Metasomatic reaction involving garnet does not necessarily imply an external source, as the core of a growth-zoned garnet is unlikely to be in equilibrium with an intergranular fluid, whether it infiltrated the rock from an external source or was generated locally by dehydration of host-rock minerals. Garlick and Epstein (1967) proposed that the similarity of O isotopic signatures between Dutchess County vein and host-rock quartz may indicate that vein quartz crystallized from a fluid in isotopic equilibrium with the host metapelites.

The timing of the fluid flow relative to metamorphism is difficult to determine, in part because most fluid inclusions are too small for microthermometric analysis. In addition, fluid inclusions in quartz veins exhibit a range of densities and compositions within single trails in host quartz, suggesting that they have been modified by deformation.

Vidale (1974) noted that vein assemblage varies as a function of metamorphic grade, with quartz veins predominating in the low-grade, western part of the sequence and quartz + plagioclase, then quartz + plagioclase + potassium feldspar to the east in the highest-grade rocks. The correlation of vein assemblage with metamorphic grade indicates that the veining event was associated with the regional metamorphism and occurred at elevated temperatures in the eastern part of the sequence.

The veins have some characteristics that suggest formation by crack-seal mechanisms (Ramsay 1980). These include slivers of wall rock incorporated into veins, but quartz crystals do not have the fibrous structure that is expected in veins that formed by successive opening and filling of cracks. The lack of fibrous crystals and the presence of crystal aggregates may indicate that the vein minerals grew from fluid-filled cracks in the presence of deviatoric stress (Wilson 1994), and that the veining was therefore syntectonic.

Textural relations combined with thermobarometric results for kyanite-zone samples place constraints on the *P-T* conditions of fluid infiltration (Whitney et al. 1996). A fluid- and mineral-inclusion–free zone near garnet rim regions follows the outline of the garnet, even around embayments, whereas the garnet core region contains what appear to be pseudosecondary trails of fluid inclusions. Pressure calculated with the GPAQ equilibria for garnet rim and embayment plagioclase compositions is ~4–5 kbar at ~525 °C. Because the textures at the garnet near-rim region represent modification of garnet that already contained fluid inclusions, fluid infiltration preceded these *P-T* conditions. Whitney et al. (1996) used thermobarometric determinations for garnet outer-core compositions to constrain infiltration conditions at 4–5 kbar and 525–550 °C. Intragarnet reaction involving fluid and mineral inclusions likely occurred at or near these conditions to create the inclusion-free zones at garnet rims. Therefore, fluid flow occurred at pressure >4 kbar, or depths of >11–12 km.

Conclusions

Fluid flow during regional metamorphism of sedimentary protoliths in Dutchess County, New York, was in part channeled along fractures and also infiltrated garnet interiors. Zoning in and around plagioclase inclusions in garnet, inclusion-free zones around mineral inclusions in garnet, and a variety of textures in garnet near-rim regions related to mineral and fluid inclusions all indicate that garnets were open to net-transfer reactions during high-grade metamorphism. This investigation suggests that modification of garnet composition was accomplished by fluid-assisted reaction during medium- to high-grade regional metamorphism, and that this process is recorded by compositional and textural features in garnet.

Acknowledgments

We thank Nick Donnelly, Jeff Walker, Timothy Grover, and Kevin Stewart for assistance with this project, and Robert Tracy, Jay Ague, and Barb Dutrow for helpful reviews.

References cited

Ague, J.J. (1994a) Mass transfer during Barrovian metamorphism of pelites, south-central Connecticut: I. Evidence for changes in composition and volume. American Journal of Science, 294, 989–1057.

——— (1994b) Mass transfer during Barrovian metamorphism of pelites, south-central Connecticut: II. Channelized fluid flow and the growth of staurolite and kyanite. American Journal of Science, 294, 1061–1134.
——— (1995) Deep crustal growth of quartz, kyanite and garnet into large-aperture, fluid-filled fractures, north-eastern Connecticut, USA. Journal of Metamorphic Geology, 13, 299–314.
Balk, R. (1936) Structural and petrological studies in Dutchess County, New York: Part I. Geologic structure of sedimentary rocks. Geological Society of America Bulletin, 47, 685–774.
Barth, T.F.W. (1936) Structural and petrological studies in Dutchess County, New York: Part II. Petrology and metamorphism of the Paleozoic rocks. Geological Society of America Bulletin, 47, 775–850.
Bence, A.E., and McLelland, J.M. (1976) Progressive metamorphism in Dutchess County, New York. New York State Geological Association Guidebook, Trip B-7.
Berman, R.G. (1990) Mixing properties of Ca-Mg-Fe-Mn garnets. American Mineralogist, 75, 328–344.
Erambert, M., and Austrheim, H. (1993) The effect of fluid and deformation on zoning and inclusions patterns in poly-metamorphic garnets. Contributions to Mineralogy and Petrology, 115, 204–214.
Ferry, J.M., and Spear, F.S. (1978) Experimental calibration of the partitioning of Fe and Mg between biotite and garnet. Contributions to Mineralogy and Petrology, 66, 113–117.
Ferry, J.M., and Dipple, G.M. (1991) Fluid flow, mineral reactions, and metasomatism. Geology, 19, 211–214.
Fisher, D.W., Isachsen, Y.W., and Rickard, L.V. (1970) Geologic map of New York, Lower Hudson Sheet. New York State Museum and Science Service Map and Chart Series 15, scale 1:250,000.
Fisher, D.W., and Warthin, A.S. (1976) Stratigraphy and structural geology in western Dutchess County, New York. New York State Geological Association Guidebook, Trip B-6.
Garlick, G.D., and Epstein, S. (1967) Oxygen-isotope ratios in coexisting minerals of regionally metamorphosed rocks. Geochimica et Cosmochimica Acta, 31, 181–214.
Hames, W.E., Tracy, R.J., Ratcliffe, N.M., and Sutter, J.F. (1991) Petrologic, structural, and geochronologic characteristics of the Acadian metamorphic overprint on the Taconide zone in part of southwestern New England. American Journal of Science, 291, 887–913.
Hames, W.E., and Menard, T. (1993) Fluid-assisted modification of garnet composition along rims, cracks, and mineral inclusion boundaries in samples of amphibolite facies schists. American Mineralogist, 78, 338–344.
Hodges, K.V., and Spear, F.S. (1982) Geothermometry, geobarometry, and the Al_2SiO_5 triple point at Mt. Moosilauke, New Hampshire. American Mineralogist, 67, 1118–1134.
Hodges, K.V., and Crowley, P.D. (1985) Error estimation and empirical geothermobarometry for pelitic systems. American Mineralogist, 70, 702–709.
Koziol, A.M., and Newton, R.C. (1988) Redetermination of the anorthite breakdown reaction and improvement of the plagioclase-garnet-Al_2SiO_5-quartz geobarometer. American Mineralogist, 73, 216–223.
Kretz, R. (1983) Symbols for rock-forming minerals. American Mineralogist, 68, 277–279.
Loomis, T.P., Ganguly, J., and Elphick, S.C. (1985) Experimental determination of cation diffusivities in aluminosilicate garnets: II. Multicomponent simulation and tracer diffusion coefficients. Contributions to Mineralogy and Petrology, 90, 45–51.
McLelland, J.M., and Fisher, D.W. (1976) Stratigraphy and structural geology in the Harlem Valley, S.E. Dutchess County, New York. New York State Geological Association Guidebook, Trip C-7.
Ramsay, J.G. (1980) The crack-seal mechanism of rock deformation. Nature, 284, 135–140.
Ratcliffe, N.M., and Burton, W.C. (1990) Bedrock geology of the Poughquag Quadrangle, New York. U.S. Geological Survey, GQ 1662.
Rumble, D. (1989) Evidence for fluid flow during regional metamorphism. European Journal of Mineralogy, 1, 731–737.
Tracy, R.J. (1982) Compositional zoning and inclusions in metamorphic minerals. In Mineralogical Society of America Reviews in Mineralogy, 10, 355–397.
Tracy, R.J., Rye, D.M., Hewitt, D.A., and Schiffries, C.M. (1983) Petrologic and stable-isotopic studies of fluid-rock interactions, south-central Connecticut: I. The role of infiltration in producing reaction assemblages in impure marbles. American Journal of Science, 283-A, 589–616.
Vidale, R.J. (1973) Metamorphic differentiation layering in pelitic rocks of Dutchess County, New York. In A.W. Hoffman, B.J. Giletti, H.S. Yoder, Jr., and R.A. Yund, Eds., Geochemical transport and kinetics, p. 273–286. Carnegie Institution of Washington, Publication 634.
——— (1974) Vein assemblages and metamorphism in Dutchess County, New York. Geological Society of America Bulletin, 85, 303–306.
Whitney, D.L. (1991) Calcium depletion halos and Fe-Mn-Mg zoning around faceted plagioclase inclusions in garnet from a high-grade pelitic gneiss. American Mineralogist, 76, 493–500.
Whitney, D.L., and Ghent, E.D. (1993) Prograde reactions and garnet zoning reversals in staurolite-schist, British Columbia: Implications for accurate thermobarometric interpretations. Journal of Metamorphic Geology, 11, 779–788.
Whitney, D.L., Mechum, T.A., Dilek, Y., and Kuehner, S.M. (1996) Progressive metamorphism of pelitic rocks from protolith to granulite facies, Dutchess County, New York: Constraints on the timing of fluid infiltration during regional metamorphism. Journal of Metamorphic Geology, in press.
Wilson, C.J.L. (1994) Crystal growth during a single-stage opening event and its implications for syntectonic veins. Journal of Structural Geology, 16, 1283–1296.
Yardley, B.W.D., and Bottrell, S.H. (1992) Silica mobility and fluid movement during metamorphism of the Connemara schists, Ireland. Journal of Metamorphic Geology, 10, 453–464.

Manuscript received April 10, 1995
Manuscript accepted January 8, 1996